VILNIUS TECH
Vilnius Gediminas Technical University

AVIATION

RATIONAL CONTROL BY TEMPERATURE IN VORTEX ENERGY SEPARATOR UNDER DESTABILIZING EFFECTS

Anatoly KULIK ⓘ, Kostiantyn DERGACHOV ⓘ, Sergiy PASICHNIK ⓘ, Dmytro SOKOL ⓘ ✉

Department of Aircraft Control Systems, National Aerospace University "Kharkiv Aviation Institute", Kharkiv, Ukraine

Abstract. The focus of this study is the arrangement of a rational control technique used to maintain the airflow temperature in a vortex energy separator (VES) under destabilizing effects. The objectives include the development of tools for the rational control of temperature in the cold and hot air flows of a VES. Methods used: Discrete state space, production rule statement, resolution of two-valued predicate equations, dichotomous trees, diagnosis, and recovery of dynamic objects. Problems settled: the studied features of the vortex energy separation process, architecture, and operation links of the rational control system were considered, mathematical models were deduced, and tools for diagnosing and recovering the efficiency of the vortex energy separator as a rational control object were developed. The scientific novelty of the study lies in the formation of instrumental tools to provide rational control of the airflow condition in the VES, where the control object is subjected to the substantial influence of various destabilizing effects.

Introduction

The intensive development of technosphere has had an increasing influence on the processes in the biosphere. It could reduce the destabilization of the biosphere in the energy sector by saving energy and increasing the environmental friendliness of energy technologies. One of these technologies is associated with the use of the vortex effect for energy separation of gases in vortex streams. Devices that realize this effect are known as vortex energy separators (VESs).

VESs are widely used in various technological fields for cooling, air conditioning, and gas and liquid separation systems. Therefore, trigenerative energy storage systems that operate in compressed air are promising. Storing air in high-pressure tanks is accompanied by high throttling losses. To reduce the losses, vortex tubes can be used to convert part of the excess pressure into useful heating and cooling of the flows (Beaugendre et al., 2021). In addition, vortex tubes can generate liquid carbon dioxide from the atmospheric air as an additional byproduct.

The ability of vortex tubes to form hot and cold gas flows can be exploited to preheat hydrogen in electric vehicles powered by hydrogen fuel cells. Heating is essential for a safe cold-start process; however, the current heating methods are energy-intensive. Alternatively, hydrogen can be heated using vortex tubes to separate compressed hy-

drogen into low- and high-enthalpy streams and using a heat exchanger to extract heat from the environment into a cold stream (Lagrandeur et al., 2023). This system uses only the excess pressure available in the hydrogen tank as the driving force. For hydrogen stored at −30 °C, the vortex tubes can increase the hydrogen supply temperature from −1.6 °C (Joule-Thompson heating in an isenthalpic choke valve) to 18.3 °C, corresponding to a heating power of 622 W.

Air separators are installed in the air intakes of helicopter engines to remove any harmful dust from the incoming air. Their use is necessary under desert conditions to eliminate the risk of rapid engine wear and the subsequent loss of power. However, their use results in an inherent loss of inlet pressure and auxiliary power in some cases. There are three main technologies: vortex tubes, barrier filters, and integrated inlet particle separators. Bazgir and Nabhani (2018) numerically studied a vortex tube. This study was conducted using the number and axial angles of inlet nozzles. The results of the numerical simulation demonstrated that the numerical model could predict the phenomenon of vortex separation inside a Ranque-Hilsch vortex tube with various geometric parameters.

Based on an analysis of the numerical and experimental modeling of the working process of vortex tubes, common characteristics of various designs were revealed (Piralishvili et al., 2017). The areas of expedient use of the

effect in engineering and technology are considered, and the prospects of creating burners, combustion chambers based on vortex flows, the use of small pipes for temperature control systems, and thermal protection against overheating and icing are shown.

The simple design and possibility of temperature separation of the inlet stream make it possible to use a VES to produce cold air in air conditioning systems. This system is environmentally friendly because no refrigerant is used in its working process (Kim et al., 2020). Experimental studies of the physical model of the air-conditioning system with VES in the variants with direct and indirect heat exchange established that the temperature during indirect heat exchange was higher than that during direct heat exchange; however, the direct heat exchange method had low hydraulic resistance.

Owing to their unique hydrodynamic properties, vortex flows are widely used in many industrial applications, including the power industry and power systems such as combustion chambers, vortex fuel atomizers, heat exchangers, cleaning systems, and drying chambers (Khalatov & Nam, 2004).

The vortex tube can provide significant performance improvement opportunities for refrigeration systems using the Joule-Thomson cycle, and it can operate efficiently at lower pressure drops with smaller recuperative heat exchangers and less expensive working fluids than those currently used (Nellis & Klein, 2002).

A serious problem for deep underground mines in tropical regions is the high temperatures at the bottom. In some cases, the airflow from the primary ventilation and central cooling systems is insufficient to provide acceptable temperature conditions. An inexpensive and maintenance-free spot-cooling system with a vortex tube powered by compressed air can be operated with or without a central cooling system (Dumakor-Dupey, 2021). Simulation results indicate that the mine can achieve a decent temperature decrease from 28 °C to 24 °C with 20 vortex tubes in the face.

The use of a vortex tube in hydrogen liquefaction plants can improve the volumetric efficiency of a liquid hydrogen pump by 20% because of vapor separation and subcooling; reduce the liquid hydrogen storage tank boil-off loss by 20% because of thermal steam shielding; increase the isentropic efficiency from 31% in the temperature range of 40–50 K to more than 40% (Leachman et al., 2020).

Vortex tubes can be used to improve the overall efficiency of power systems, particularly micropower systems. For example, a vortex tube was considered in combination with a waste heat steam generator (Arslan et al., 2002). The vortex tube separates the turbine exhaust stream into hot and cold streams. The cooler stream was sufficiently hot to supply all the heat required for the economizer section, leaving the hotter stream to increase the temperature at the outlet of the superheater. Thus, the air leaving the waste heat boiler and entering the steam turbine has an increased enthalpy, and the efficiency of the cycle improves. In addition, the output quality of the steam turbine is improved.

Vortex energy separators are also used in aviation. Thus, in the aerospace industry, it is impossible to use liquid cooling of the cutting zone owing to the specific properties of the material or the design features of the workpiece. The use of a vortex tube allows cold air to be supplied to the cutting zone. This prevents chips from adhering to the cutting edge of the tool (Belov et al., 2018). VESs were developed for the individual conditioning of the pilot suit (Merkulov, 1992). VESs have been successfully used as cooling blocks for onboard electronic equipment on an aircraft, in anti-icing systems (Biryuk et al., 2021), and in air conditioning systems for aircraft cabins (Barbonov et al., 2017).

During operation, VESs are subjected to various destabilizing effects such as onboard temperature and pressure fluctuations, compressed air parameter changes, and output air flow load variations. Moreover, under the harsh conditions of autonomous use, the inevitable degradation of VES components leads to a significant deterioration in operational efficiency and even failures. Classical principles and instrumental tools for automatic control do not ensure the operability of VES under diverse destabilizing effects.

The classical principles and tools of automatic control do not ensure the operability of VES under diverse types of destabilizing effects. The scientific and technical problem is to effectively ensure the operability of the VES under various types of destabilizing effects under onboard, long-term, and autonomous operation conditions. A possible solution to this problem is to use new control principles and rational control tools based on production knowledge bases and inference structures (Kulik, 2016).

In this study, the results of the development of rational control tools for a class of linearizable VES under the influence of different types of destabilizing effects are presented. Section 1 describes the device and principle of operation of the VES. Section 2 presents the features and structure of a sustainable renewable energy management system. For rational control, a VES must have properties that ensure the diagnosability and recoverability of its performance. The diagnostic software used to implement the diagnostic process is presented in Section 3. Furthermore, in Section 4, the procedures for restoring the operability of the VES using functional diagnostic models that link the deviations of the signals available for measurement (indirect features) with the deviations of the parameters of the mathematical models (direct features) are described. Section 5 presents the results of a computer simulation of a rational control system of a VES for 23 kinds of destabilization effects.

1. Vortex energy separator

A VES is a gas-dynamic generator of cold and hot air that applies the potential energy of a precompressed gas (Merkulov, 1992). Owing to the effect of temperature separation in the twisting gas flow, the conversion of thermal energy occurs in the VES. A schematic representation of the VES is shown in Figure 1 (Kulik et al., 2021).
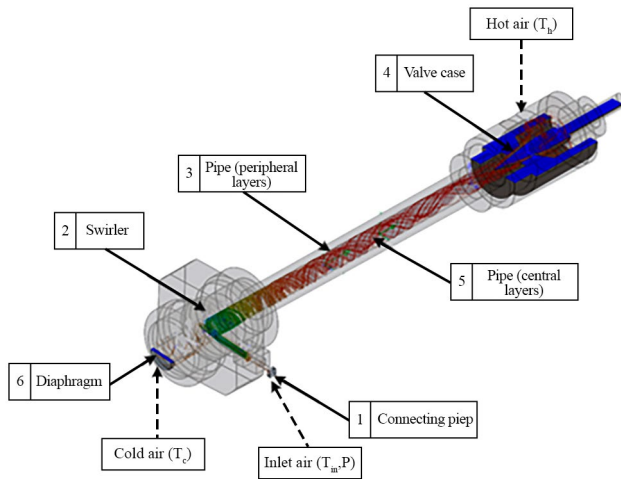
Figure 1. VES device arrangement: 1 – intel nozzle; 2 – twisting device; 3 – energy separation chamber; 4 – crosspiece; 5 – cone valve; 6 – diaphragm

The operating principle of the VES is as follows (Figure 1). Compressed gas with pressure P enters nozzle device inlet 1, which is a smooth tapering channel of a rectangular cross-section, in which the gas flow is given rotational motion owing to the spiral shape of twisting device 2. The most common form of the spiral is the Archimedes spiral, which provides the smoothest change in the velocity-vector direction. The twisted gas flow enters energy separation chamber 3 and then moves by a helical trajectory within the near-wall area to the straightening crosspiece and next to cone valve 4. Passing through the crosspiece, the gas flow loses its circumferential velocity component, resulting in a slight increase in pressure. The flow area of the cone valve was not sufficient for the passage of all the gas masses. Therefore, part of the flow moved in the opposite direction from valve 5, namely, in the axial area of energy separation chamber 3, and discharged through diaphragm 6.

Energy exchange occurs when moving in opposite directions; as a result, the peripheral layers are heated and the paraxial layers are cooled. Thus, the temperature of the gas that leaves energy separation chamber 3 through cone valve T_h becomes higher than the temperature of the gas, which supplies the VES, T_{in} Accordingly, the exiting diaphragm gas flow had a lower temperature, T_c, than the gas at Inlet 1.

The processes occurring in the VES in both steady-state and transient modes are characterized by various features.

- A peripheral flow is a large-scale vortex structure with developed turbulence that moves according to the law of free vortices.
- The paraxial flow has a small-scale turbulent structure and moves in the energy-separation chamber according to the forced vortex law.
- The distribution of the thermodynamic and kinematic parameters of the vortex flows in the volume of the chamber was significantly uneven.
- Regime parameters of the VES are sensitive to changes in both the internal and external operating conditions.
- Significant dependence of rotating flow parameters on design features and operating conditions of VES.

The listed features of the effect of temperature separation, as well as the insufficient knowledge of the nature of this phenomenon, do not allow one to analytically form a mathematical model of the VES as an object of automatic control.

The significant nonlinearity of the VES static characteristics, distribution of parameters, and their nonstationarity in steady-state and transient conditions necessitate the use of adaptive control of the state of a rotating gas flow to achieve the performance quality required in various technical applications.

2. Features of the rational control

Rational control is based on the hypothesis of uncertainty of destabilizing effects. This means that the uncertainties are moments when destabilizing effects arise, and the place of destabilization, its type, and magnitude are unknown. It is also assumed that only one destabilizing effect can appear at a certain point in time (Kulik, 2016).

The presented research is a deepening and practical specification of the paper (Kulik et al., 2022a), which is focus on of theoretical studies of the possibility of rational control of the vortex energy separator under conditions of various destabilizations. However, due to the stage of computer simulation in this article, the rational control system structure was enhanced.

With regard to the problem of automatic VES control, rational control aims to determine the relationship between the two subsystems. The first subsystem identifies
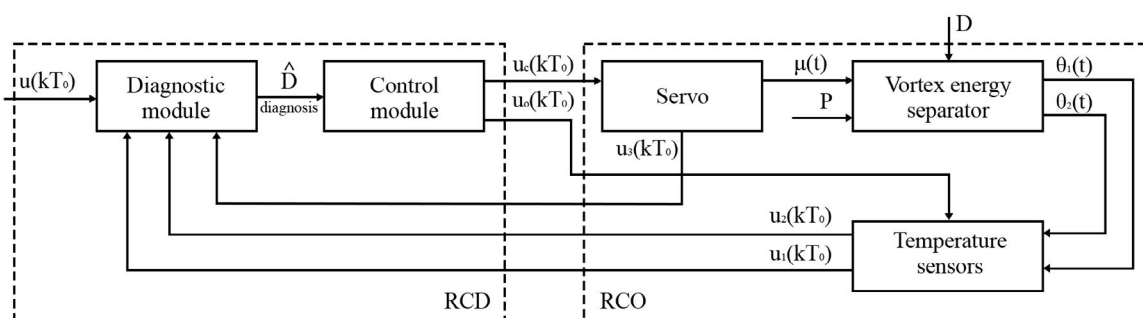
Figure 2. Functional diagram of the rational control system

a rational control object (RCO), the second implies a rational control device (RCD), and the appropriate functional signal links aggregate them. Figure 2 shows a functional diagram of the rational control system (Kulik et al., 2022a).

The RCO involves the control object, VES, to which compressed air receiving pressure P is supplied, a servo unit that governs the cone valve position $\mu(t)$ in the energy separation chamber, and temperature sensors for cold $\theta_1(t)$ and hot $\theta_2(t)$ air flows. The RCO subsystem is affected by a set of uncontrolled destabilizing actions D assumed to present uncertain events.

RCD includes diagnostic and control software modules. The diagnosis module determines the VES functional state in the form of an estimate $\hat{D}$ of the destabilizing effect features. The module relies on the available signals from dedicated sensors: the servo's signal $u\left(kT_0\right)$, signals from the temperature sensors of cold $u_1\left(kT_0\right)$ and hot $u_2\left(kT_0\right)$ airflows, and a signal from the control valve position sensor $u_3\left(kT_0\right)$. The control module generates control impacts $u_c\left(kT_0\right)$ and $u_o\left(kT_0\right)$ on the RCO, which respond to the RCO functioning recovery based on the results of its diagnosis. Here and there k is a discrete step number, T_0 is sampling time.

The key element in the presented functional diagram is the diagnostic module aimed at assessing the RCO condition. It is necessary to detect the occurrence of the destabilizing effect, localize and identify the effect by searching for the impacted functional elements, and determine their type, followed by specific recognition.

The detection of the destabilizing effect is the establishment of a fact for incorrect RCO running. Localization refers to the search for a functional element that has been subjected to destabilizing influences. The diagnosis type contributes to the group of destabilizing influences, resulting in the same disruption features of RCO performance. The destabilizing effect refers to its specific physical manifestation, which could be eliminated with the help of available recovery resources. Thus, the diagnostics module supplies a procedure that is a sequential process for establishing the fact of destabilization, searching for the place of its occurrence, identifying the type, and determining the specific kind of destabilizing effect.

In the presented functional diagram (Figure 2), the RCO differs from conventional classic automatic control objects. The RCO can supply the diagnosability and recoverability of its performance in addition to the conventional properties of controllability and observability. Diagnosability is a property that consists of the ability to unambiguously set the cause of the destabilizing effect in finite time and use the available measurement signals. It is evaluated using the criteria of structural and signal diagnostic ability. Restorability is a property of the RCO that makes it possible to fend off destabilizing effects in finite time using hardware and software facilities. It is assessed using a special recoverability criterion, which allows one to form a sufficient resource to parry the set D of the destabilizing impacts of different types.

Rational control was implemented as a reasonable combination of analytical methods and computational, mockup, and experimental workbench studies.

3. Diagnosis of the rational control object

Appropriate support was provided for implementation of the diagnostic process. The diagnostic support of the RCO consists of mathematical models that describe the nominal operation mode of the functional elements and the entire control object, diagnostic models relating the direct and indirect features of the diagnosis, computational algorithms recognizing direct and indirect features, and predicate equations that rest on the dichotomous branches of the diagnosis tree (Kulik et al., 2022b).

In the nominal operation mode, which exhibits destabilizing effects, the RCO is depicted in the block diagram shown in Figure 3. The sampling time, T_0 in the variable argument for signal samples is not shown to simplify this notation.

Other characters mean the following: $u_c\left(k\right)$ – control signal sample value, $x_1\left(k\right)$ – state variable of the servo, $x_2\left(k\right)$ – state variable of the VES cold airstream channel, $x_3\left(k\right)$ – state variable of the cold air temperature sensor, $x_4\left(k\right)$ – state variable of the VES hot airstream channel, $x_5\left(k\right)$ – state variable of the hot air temperature sensor, $u_1\left(k\right)$ – cold airstream temperature sensor output, $u_2\left(k\right)$ – hot airstream temperature sensor output,

Figure 3. Block diagram of the RCO in the discrete state space

$u_3(k)$ – valve's position sensor output, κ_1 – servo gain, κ_2 – VES cold airstream channel gain factor, κ_3 – gain of the cold air temperature sensor, κ_4 – VES hot airstream channel gain factor, κ_5 – gain of the hot air temperature sensor, κ_1' – displacement sensor gain, T_2 – VES cold airstream channel time constant, T_3 – time constant of the cold air temperature sensor, T_4 – VES hot airstream channel time constant, T_5 – time constant of the hot air temperature sensor.

Different types of destabilizing impacts result in disturbances in the RCO performance, which means a change in the gain factors, time constants, and zero-drift appearance (Kulik, 2016). Consequently, it is necessary to form a set *D* of the destabilization effects representing the deflections of the gains, time constants, and signal values.

The implementation of RCO diagnosis strategy involves the successive settling of the following tasks:

- detection of destabilization;
- search for the location of the functional element impacted by destabilization;
- settling the type of destabilizing effect;
- determination of the disturbance kind;
- arrangement of the diagnosis dichotomous tree.

The dichotomous tree is the production knowledge base containing RCO operation failures, and this knowledge logical relationship structure is used to diagnose the cause of malfunctions that occur during transient process times in real time.

Using two-valued dichotomous equations, an inference was made on logical variables that exposed diagnostic features for the RCO functional condition. When the logical relationship between features is known, they can be systematized in the form of a dichotomous tree, as shown in Figure 4 (Kulik et al., 2022a).

Consider the process of forming the diagnosis on a specific example.

Let the RCO be impacted by a disturbance that manifests itself as a zero drift of the servo, x_{10}, i.e., a destabilization of kind d_3 has gone.

The detection function establishes a disturbance during RCO operation. The RCO reference model is used to solve this problem; the sample should be displayed in digital form in the nominal operation mode

$$\hat{x}\left[(k+1)T_0\right] = \mathbf{A} \cdot \hat{x}(kT_0) + \mathbf{b} \cdot u_c(kT_0);$$
$$x(0) = x_0; \tag{1}$$
$$\hat{u}(kT_0) = \mathbf{C} \cdot \hat{x}(kT_0),$$

where $\hat{x}(kT_0)$ is the vector for RCO's reference state, $\hat{u}(kT_0)$ is the reference measurement vector, $\mathbf{A}$, $\mathbf{b}$, and $\mathbf{C}$ are system matrices of the corresponding dimension.

Measurement vector $\tilde{u}(kT_0)$ changes when a destabilizing effect appears in the RCO. This change is consolidated with the predicate equation

$$z_0 = S_2\left\{|\tilde{u}(kT_0)| - |\hat{u}(kT_0)| \geqq \delta_0\right\};$$
$$k = \overline{k_1, k_2}, \quad p, \tag{2}$$

where S_2 is denotes the two-valued predicate, δ_0 is the tolerance value, and p is the confidence coefficient.

Hence, the inference rule is written as

$$z_0 = \begin{cases} 1, & \text{if } \left|\Delta u(kT_0)\right| \geq \delta_0; \\ 0, & \text{if } \left|\Delta u(kT_0)\right| < \delta_0, \end{cases} \tag{3}$$

Figure 4. Dichotomous diagnosis tree

where $\Delta u(kT_0) = \tilde{u}(kT_0) - \hat{u}(kT_0)$, the true z_0 denotes the presence of destabilization, and false z_0 indicates no destabilization.

Confidence coefficient p is used to exclude erroneous or affected noise meanings of the discrete deviation, $\Delta u(kT_0)$; thus, the decision-making in Equation (3) is disturbed.

The task of finding the destabilization location is solved only for RCO components and intends to use reference models and sensor signals.

Therefore, to identify servo malfunctions, it is necessary to first handle sensor signal $\tilde{u}_3(k+1)$ and the reference model signal

$$\hat{u}_3(k+1) = \hat{u}_3(k) + \kappa_1 T_0 u_c(k) \tag{4}$$

and then treat their distinction according to the predicate equation

$$z_1 = S_2\left\{\left|\Delta u_3(k+1)\right| \geq \delta_1\right\};$$
$$k = \overline{k_2, k_3}, \ p, \tag{5}$$

where $\Delta u_3(k+1) = \tilde{u}_3(k+1) - \hat{u}_3(k+1)$.

Hence, the inference rule record can be as follows:

$$z_1 = \begin{cases} 1, \ if \ \left|\Delta u_3(k+1)\right| \geq \delta_1; \\ 0, \ if \ \left|\Delta u_3(k+1)\right| < \delta_1. \end{cases} \tag{6}$$

Therefore, if z_1 is true, servo destabilization occurs, and a transition to z_2 is required if z_1 is false.

To identify the type of servo destabilization, it is necessary to form a functional diagnostic model that represents the relationship of indirect x_{10} and direct u_{30} destabilization features. The functional diagnostic model for zero drift is written as

$$\Delta u_3(k+1) = \Delta u_3(k) + u_{30}, \tag{7}$$

where $\Delta u_3(k)$ is the output of the servo-valve relocation sensor and u_{30} is the servo zero drift discovered by the connected position sensor.

The predicate equation for identifying the type of servo destabilization can be as follows:

$$z_{11} = S_2\left\{\left|2\Delta u_3(k+1) - \Delta u_3(k+2) - \Delta u_3(k)\right| \geq \delta_{11}\right\};$$
$$k = \overline{k_4, k_5}, \ p. \tag{8}$$

The inference for z_{11} as false indicates presence of the zero drift u_{30}. If z_{11} is true, then the type of destabilization identified is servo's gain driftage, $\Delta \kappa_1$.

The need to solve the problem of identifying the kind of destabilization is associated with various possibilities for restoring RCO performance. Destabilizing impacts can have a significant magnitude; therefore, they can be compensated for with dedicated adjustments. In this case, the parry was performed by reconfiguring the algorithms and equipment. Therefore, the compensable and non-compensable kinds of destabilizing effects are examined for the u_{30} type.

To identify a specific kind of destabilizing effect, it is necessary to determine the value of a direct feature. It is practical to use the estimated $\hat{u}_{30}$ of the current value for this purpose because it is continuously computed at each sampling interval as

$$\hat{u}_{30}(k) = \Delta u_3(k+1) - \Delta u_3(k). \tag{9}$$

If a boundary value $\overline{u}_{30}$ is set to distinguish between the two kinds, then the predicate equation is used

$$z_{110} = S_2\left\{\overline{u}_{30} \ < \ \hat{u}_{30}\right\}, \tag{10}$$

where $\hat{u}_{30}$ designates the arithmetic mean of $\hat{u}_{30}(k)$ values; it is possible to determine a particular kind of drift, namely, that would be the compensable kind d_3, if the inference z_{110} is false, and the non-compensable d_4, when z_{110} is obtained as true.

The dichotomous tree's branches for other kinds of destabilizing effects are constructed similarly.

4. Performance recovering

After receiving a complete diagnosis of the causes of RCO malfunction, it is necessary to proceed to the next procedure of rational control, which assumes performance recovery. Recovery actions are arranged using functional diagnostic models that link the deviations of signals available for measurement (indirect features) with the deviations of the mathematical model parameters (direct features). By solving inverse problems, a control action that fends off the identified kinds of destabilizing effects is formed.

The following excess methods are used when recovering the RCO operability: signal adjustment, parametric tuning, algorithm rearrangement, and hardware reconfiguration. Consider the performance recovery features of the following servo example:

According to Figure 4, four kinds of destabilizing effects $d_1 \div d_4$ fall under servo diagnosis. A compensable kind, when appearing as a zero-drift u_{30} can be fended off by a signal trim. The extent of this adjustment was determined according to the following functional diagnostic model:

$$\tilde{x}_1(k+1) = \tilde{x}_1(k) + \kappa_1 T_0 u_c(k) + \frac{u_{30}}{\kappa_1'}. \tag{11}$$

The condition for zero-drift compensation yields

$$\kappa_1 T_0\left[u_c(k) + u_c'(k)\right] + \frac{u_{30}}{\kappa_1'} = \kappa_1 T_0 u_c(k), \tag{12}$$

from which the compensating signal can be found to be

$$u_c'(k) = -\frac{\hat{u}_{30}}{\kappa_1' \kappa_1 T_0}. \tag{13}$$

In Equation (13), $\hat{u}_{30}$ is the estimate of the zero drift value determined using Equation (9).

When noncompensable kind d_4 occurs in the servo, it is necessary to replace the faulty servo with a backup servo to restore the RCO performance.

5. Fragment of computer simulation results

Using Simulink, a computer simulation of the VES rational control system was performed for 23 kinds of destabilization effects. The following parameters were used in the case study: κ_1 = 1.8 mm/V, κ_2 = −10.16 ^{0}C/mm, κ_3 = 0.1 V/^{0}C, κ_4 = −26.28 ^{0}C/mm, κ_5 = 0.11 V/^{0}C, κ_1' = 0.55 V/mm, T_2 = T_4 = 8 sec, T_3 = 0.1 sec, T_5 = 0.11 sec, T_0 = 0.001 sec.

Figure 5 shows the waveforms that display the process of servo performance diagnosis and recovery when destabilization manifests itself as a compensable zero drift in servo d_3.

A control test signal u_c in the form of a pulse of 0.1 V and Δt = 1.5 s duration was applied at the servo input (Figure 5a), thus actuating the valve at the the t = 1 s instant. The valve movement (Figure 5b) consequent response of the RCO changes the output of the components, including the voltage of the cold airstream temperature sensor, as shown in Figure 5h.

At time t = 3 s, the assay signal of a servo zero drift −0.2 V is added (Figure 5c). This disturbance is reflected in the cone–valve displacement (Figure 5b). This destabilizing effect was detected at t = 3.4 s using predicate Equation (2) (Figure 5d). After RCO destabilization is detected, the fault functional element is found, namely, the servo, using the predicate z_1 (Figure 5e). The type of fault was determined using the predicate z_{11} (Figure 5f) and its kind using the predicate z_{110} at time t = 3.7 s (Figure 5g). The entire process of diagnosis Δt

lasts 0.7 s, which can be observed from the graph for the valve motion response (Figure 5b). At t = 3.8 s, the signal adjustment originates as a pulse impact of 0.1 V and Δt = 1.2 s length that is added to the principal control action (Figure 5a).

The servo performance was recovered by t = 5 s (Figure 5b) and RCO performance recovery continued until t = 12 s (Figure 5d); false inference of the predicate z_0 states the end of the recovery process.

In the case study, the diagnostic interval was Δt_d = 0.7 s and the recovery time was Δt_r = 10.3 s. After recovery completion, the difference between the RCO output and the reference model was less than 5%. The time from the moment of servo destabilization to RCO recovery was Δt_f = 9 s, and the settling time of the reference model was Δt_t = 11 s. Thus, the RCO completes its normal performance restoration within a given transient object time. The relative error in the RCO response throughout the steady state is 1.3%.

The influence of other compensable destabilizations was simulated similarly. The diagnosis was successful, and the RCO performance recovered. The maximum relative error through the simulated destabilizing influences was attributed to d_7 and was equal to 7.5%.

The results of the destabilization process modeling for all compensable effects on the set D (Figure 4) conducted with the provision of their diagnosis and following compensation show the fundamental possibility of handling the VES rational control in the presence of a destabilizing influence.
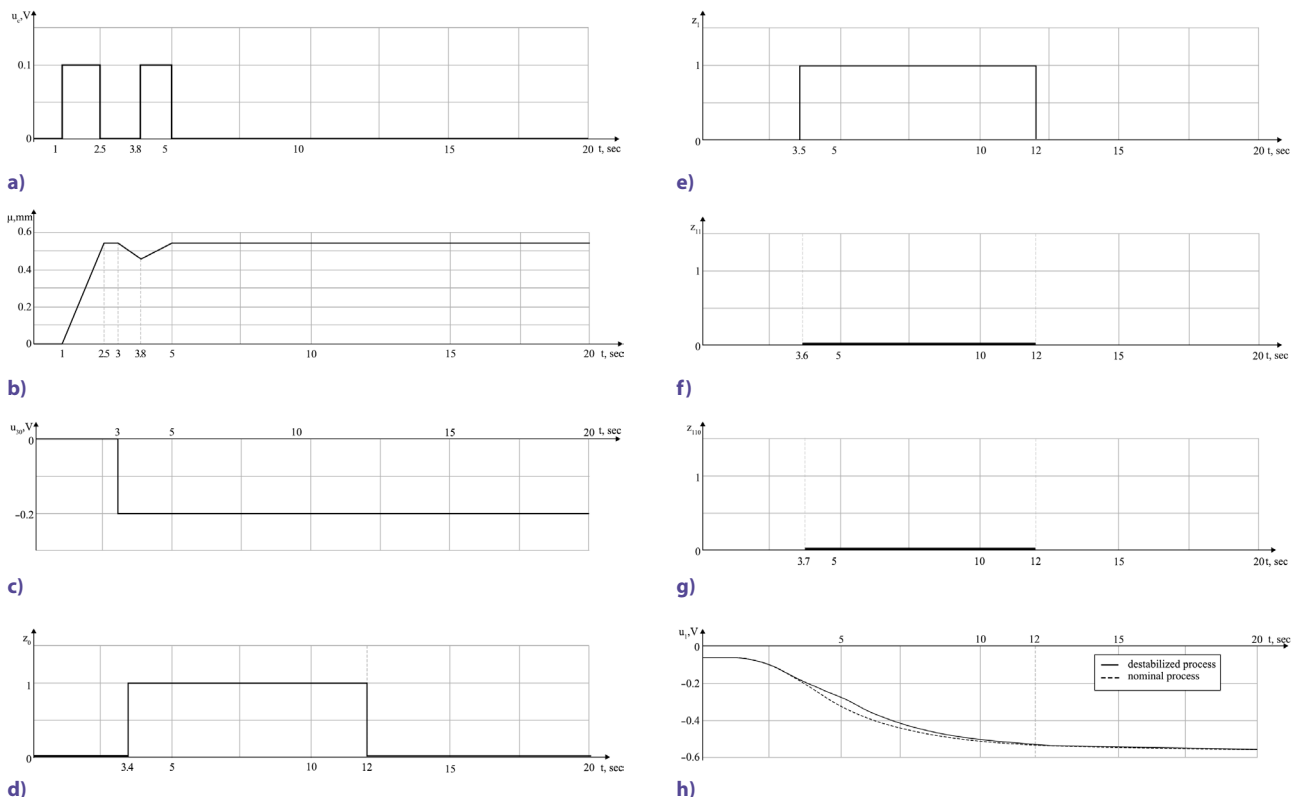
Figure 5. VES servo malfunction diagnosing and RCO performance restoration

Conclusions

In this study, new mathematical models of the VES as an object of automatic control in a discrete space of states were obtained. The mathematical models reflect the processes of signal conversion in the nominal and emergency modes owing to different types of destabilizing effects. The obtained mathematical models make it possible to analytically solve the problems of synthesizing procedures for the rational control of the VES.

The new result is the resulting dichotomous tree, which is a knowledge base of the emergency modes of the VES as an object of automatic control, and the structure of a logical conclusion regarding the causes of destabilization. The proposed tools can be used to form knowledge bases and inference structures for other VES classes.

New means of parrying out different types of destabilizing influences are investigated: signal and parametric adjustments and reconfiguration of algorithms and equipment, which creates new opportunities for solving problems of flexible control of redundant means to extend the period of active operation of autonomous VES.

The results of the computational experiment indicate the fundamental possibility of prompt diagnosis and flexible restoration of the operability of the VES as an object of automatic control, i.e., through rational control. The speed of the rational control of the VES on average was Δt_f = 9 s, which was less than the speed of the automatic control object itself, Δt_t = 11 s. The average recovery accuracy is 1.3%.

The results of this study enables the development of automatic control systems for VESs that allow them to function effectively and autonomously under the influences of noise, interference, changes in environmental characteristics, malfunctions, failures, failures, and other destabilizing effects.

The developed mathematical models and tools for diagnosing and restoring operability can be used in the development of the effective control of VESs used as part of airborne systems for long periods of autonomous operation.

Disclosure statement

The authors declare to have no competing financial, professional or personal interests from other parties.

Author contributions

Anatoly and Kostiantyn conceived the study and were responsible for the design and development of the data analysis. Sergiy was responsible for data collection and development of mathematical models. Dmytro was responsible for computer simulation and data interpretation. Dmytro wrote the draft of the article.

References

Arslan, S., Mitrovic, B., & Muller, M. R. (2002). Vortex tube applications in micro-power generation. In *International Joint Power Generation Conference*. Scottdale, Arizona, USA. https://doi.org/10.1115/IJPGC2002-26056

Barbonov, E. O., Biryuk, V. V., Gajnullin, M. N., Sotova, V. A., & Chertykovtsev, P. A. (2017). The hybrid cooling system of onboard infrared detectors on the basis of vortex and thermoelectric effects. *Vestnik mezhdunarodnoi akademii kholoda*, *2017*(2), 31–37. https://doi.org/10.21047/1606-4313-2017-16-2-31-37

Bazgir, A., & Nabhani, N. (2018). Numerical investigation of the effects of geometrical parameters on the vortex separation phenomenon inside a Ranque-Hilsch vortex tube used as an air separator in a helicopter's engine. *Aviation*, *22*(1), 13–23. https://doi.org/10.3846/aviation.2018.2414

Beaugendre, E., Lagrandeur, J., Cheayb, M., & Poncet, S. (2021). Integration of vortex tubes in a trigenerative compressed air energy storage system. *Energy Conversion and Management*, *240*, 114225. https://doi.org/10.1016/j.enconman.2021.114225

Belov, G. O., Dostovalova, S. S., Barbanov, E. O., Uglanov, D. A., Chertykovtsev, P. A., & Panshin, R. A. (2018). The Vortex air-cooler system for cutting materials in aerospace industry. *MATEC Web Conferences*, *179*, 02007. https://doi.org/10.1051/matecconf/201817902007

Biryuk, V. V., Lukachev, S. V., Volov, V. T., & Pirallishvili, Sh. A. (2021). Professor Merkulov role in the process of research and development of the vortex effect. *Vestnik of Samara University. Aerospace and Mechanical Engineering*, *20*(2), 105–121. https://doi.org/10.18287/2541-7533-2021-20-2-105-121

Dumakor-Dupey, N. K. (2021). *Application of vortex tubes in an underground mine ventilation system*. University of Alaska.

Khalatov, A. A., & Nam, Ch.-D. (2004). Aerothermal vortex technologies in aerospace engineering. *Journal of the Korean Society of Marine Engineers*, *28*(2), 163–184.

Kim, Y., Im, S., & Han, J. (2020). A study on the application possibility of the vehicle air conditioning system using vortex tube. *Energies*, *13*(19), 5227. https://doi.org/10.3390/en13195227

Kulik, A. S. (2016). *Elementyi teorii ratsionalnogo upravleniya ob'ektami*. National Aerospace University "Kharkiv Aviation Institute" (in Russian).

Kulik, A., Dergachov, K., Pasichnik, S., & Sokol, D. (2022a). Rational control of the temperature of vortex energy separator under destabilizing influence. *Radioelectronic and Computer Systems*, (3), 47–66. https://doi.org/10.32620/reks.2022.3.04

Kulik, A., Dergachov, K., Pasichnik, S., & Sokol, D. (2022b). Diagnostic models of inoperable states of the vortex energy separator device. *Aerospace Technic and Technology*, (3), 13–29. https://doi.org/10.32620/aktt.2022.3.02

Kulik, A. S., Pasichnik, S. N., & Sokol, D. V. (2021). Modeling of physical processes of energy conversion in small-sized vortex energy separators. *Aerospace Technic and Technology*, (1), 20–30. https://doi.org/10.32620/aktt.2021.1.03

Lagrandeur, J., Uzundurukan, A., Mansour, A., Poncet, S., & Benard, P. (2023). On the benefit of integrating vortex tubes in PEMFC system for preheating hydrogen in FCEV technologies. *International Journal of Hydrogen Energy*. https://doi.org/10.1016/j.ijhydene.2022.11.246

Leachman, J., Matveev, K., McMahon, J., Eldrid, S., Bunge, C., Wallace, G., Attapattu, J., & Combs, S. (2020). *Heisenberg vortex tube for cooling and liquefaction*. Washington State University.

Merkulov, A. P. (1992). Vihrevoy effekt i ego primenenie v tehnike. *Optima* (in Russian).

Nellis, G. F., & Klein, S. A. (2002). The application of vortex tubes to refrigeration cycles. In *International Refrigeration and Air Conditioning Conference* (paper 537). Purdue University.

Piralishvili, Sh. A., Veretennikov, S. V., Piralishvili, G. Sh., & Vasilyuk, O. V. (2017). Analiz teplofizicheskih protsessov v vihrevyih trubah. *Vestnik PNIPU. Aerokosmicheskaya tekhnika*, (49), 127–141 (in Russian).